Anharmonic effects on monolayer phonons

L. W. Bruch

Department of Physics, University of Wisconsin–Madison, Madison, Wisconsin 53706

A. D. Novaco

Department of Physics, Lafayette College, Easton, Pennsylvania 18042
(Received 4 June 1999; revised manuscript received 14 October 1999)

The anharmonic frequency shifts of the phonons in monolayer solids of Ar/Pt(111) and commensurate Xe/Pt(111) are calculated with quasiharmonic perturbation theory and with self-consistent-phonon theory. Results from the two methods are in good agreement for Ar/Pt(111). Uncertainties in the frequency shifts for the Ar/Pt(111) modes are small compared to present uncertainties in the interaction model and in the experimental data. Anharmonic effects in the commensurate Xe/Pt(111) solid at 80 K are large, both because of the small adatom-adatom force constants in this dilated lattice and because of the large degree of thermal excitation. A version of the improved self-consistent-phonon approximation is used for comparison to experimental data, and it is found that the anharmonic terms cause changes on the scale of adjustments in Xe-Pt forces previously found necessary to achieve fits of the harmonic theory to the data. The contribution of static adsorption-induced dipole moments to the monolayer lattice dynamics is analyzed and is found to be negligible for Xe/Pt(111).

I. INTRODUCTION

While the theory of anharmonic processes in monolayer solid lattices has been formulated for a long time,[1,2] the actual measurement of the phonon dispersion relations for monolayers on single-crystal surfaces is a recent accomplishment.[3–8] In a few cases,[8] all three branches of the dispersion curve of a monatomic solid with one atom per unit cell have been observed. Remaining doubts[3–9] about whether to assign observed excitations to the shear horizontal (SH) or to the longitudinal acoustic (LA) branches may be reduced by precise comparisons of the observed dispersion relations with those calculated using realistic interaction models. For given interactions, the evaluation of lattice dynamics in the harmonic approximation[10] is now straightforward. However, the experiments include cases of relatively small mass adsorbates and of quite dilated lattices; in such instances, anharmonic frequency shifts and temperature-dependent lifetimes may be appreciable.[11] The two examples[12] treated in this paper, an incommensurate lattice of Ar/Pt(111) with $L \approx 3.79$ Å and the commensurate $\sqrt{3}R30°$ Xe/Pt(111) lattice with $L = 4.80$ Å, show successes and limitations of the methodology, respectively.

Inert-gas solids in three dimensions[13] and as monolayers[14] are proving grounds for the theory of dense phases because the interatomic potentials are thought to be nearly equal to those for the isolated pair determined by scattering experiments or by analysis of gas-phase data. In this context, argon solids are intensively studied because the masses are large enough that quantum effects are small while the many-body interactions, with magnitude roughly scaling as the cube of the atomic polarizability, are still small. Both features enhance the accuracy with which the theory can be implemented. The xenon solids are stable over a wider temperature range than the argon solids and have smaller quantum corrections. Although the many-body interaction terms are

larger, lattice dynamics in the harmonic approximation is accurate for the three-dimensional (3D) xenon solid. However, the applicability of these ideas to monolayer solids is in question and is invalid if the most widely observed phonon mode[3–6] is LA rather than SH.

Four different approximations, denoted QHT, QHPT, SCP, and ISCP, are used to evaluate the phonon dispersion relations. Comparison of the approximations provides a way to judge the degree of convergence of the truncated perturbation theory. Quasiharmonic theory (QHT) gives the harmonic normal mode frequencies for a thermally expanded lattice. In quasiharmonic perturbation theory (QHPT), anharmonic corrections to the QHT frequencies are evaluated with perturbation theory carried to first order $\omega_1(4)$ in the quartic and to second order $\omega_2(3)$ in the cubic anharmonic terms of an expansion of the adlayer potential energy in displacements from the average lattice sites,

$$\omega(\text{QHPT}) = \omega(\text{QHT}) + \omega_1(4) + \omega_2(3). \qquad (1.1)$$

Another approach is the self-consistent-phonon (SCP) approximation, which retains all even-order terms in the displacement expansion. The improved self-consistent-phonon theory (ISCP) forms final frequencies by adding the cubic anharmonic term of the QHPT to the SCP result,[15]

$$\omega(\text{ISCP}) = \omega(\text{SCP}) + \omega_2(3). \qquad (1.2)$$

It is considered to be the most reliable form of the perturbation approach to the anharmonic effects.[2] In these approximations, the phonon lifetimes (linewidths in response functions) arise from three-phonon processes in second-order perturbation theory.

Initial comparisons of the approximations were made for the Ar/Pt(111) lattice at zero temperature. As discussed in Sec. III, the QHPT and SCP approximations were in such good agreement that the further work is based on the finite-

temperature form of the QHPT. However, the application of QHPT to the commensurate Xe/Pt(111) lattice at 80 K shows such large anharmonic terms that the comparisons to the experimental data are based on the ISCP approximation.

The organization of this paper is as follows. Section II contains a description of the components of the calculation. Section III presents the application to Ar/Pt(111) and Sec. IV the application to commensurate Xe/Pt(111). Concluding remarks are given in Sec. V. The contribution of polarizable adatom dipole moments to the elastic constants of a triangular lattice is estimated in the Appendix. Supplementary material has been deposited in the EPAPS archive.[16]

II. COMPONENTS OF THE CALCULATION

A. Structures and interactions

The triangular Ar/Pt(111) lattice is approximated as a floating unmodulated monolayer solid, and the lattice constant $L = 3.79$ Å is that corresponding to the recent inelastic helium atom scattering (HAS) measurements[8] at 23 K. The only parameter of the adatom-substrate potential required for the calculations is the frequency $\omega_{0\perp}$ of the vibration perpendicular to the monolayer plane at zero wave number, taken from the HAS experiments to be $\omega_{0\perp} = 4.85$ meV. The anharmonic effects all arise from the anharmonicity of the adatom-adatom potentials, which are a combination of the HFD-B2 multiparameter pair potential,[17] constructed from 3D data, and the McLachlan substrate-mediated dispersion energy. Full statements of the models and their parameters are given in Appendix A of Ref. 8.

The $\sqrt{3}R30°$ Xe/Pt(111) lattice, with $L = 4.80$ Å, is greatly dilated from the usual range for xenon lattice constants, 4.4–4.6 Å. The Xe-Xe potential is constructed in analogy to that used for Ar-Ar. Contributions of adsorption-induced xenon dipole moments are omitted from the calculated dispersion curves as estimates presented in the Appendix show them to be less than 0.1 meV throughout the Brillouin zone. The Barker-Rettner model[18] is used for the Xe-Pt potential. Anharmonicity of the Xe-Pt interaction makes major contributions to the anharmonic shifts of the normal mode frequencies.

B. Estimating anharmonic effects

The data for the Ar/Pt(111) monolayer solid are at low enough temperatures so that effects of thermal expansion in the z coordinate are anticipated to be small. The SCP calculation for Ar/Pt(111) is at zero temperature and follows procedures outlined in Ref. 1. The effects of finite temperature are estimated at $T = 23$ K using the QHPT formalism;[16,19] resonant energy denominators in the second-order perturbation terms are treated with the Lorentzian approximation [half width at half maximum (HWHM) ≈ 0.005 meV] used by Hall et al.[20] For Ar/Pt(111), the perpendicular motion decouples from the in-plane motion and the calculation of the in-plane modes is done for mathematical 2D.

The phonon data for the $\sqrt{3}R30°$ Xe/Pt(111) lattice are[7] at 80 K, and thermal effects should be included when comparing to data for the incommensurate monolayer solid with $L \approx 4.33$ Å at 50 K (Ref. 8) and 25 K (Ref. 20) or to data for the 2D gas near 100 K (Refs. 8 and 21). Thermally driven

TABLE I. Comparison of values from quasiharmonic perturbation theory (QHPT) and self-consistent perturbation (SCP) theory for commensurate Xe/Pt(111). Overlayer heights z in Å and zone-center, Γ-point, frequencies ω_0 in meV. $\parallel$ and $\perp$ denote motions parallel and perpendicular to the monolayer plane, respectively. The dispersion $\Delta\omega_\parallel$ is given for in-plane modes from the Brillouin zone Γ point to the K point, $Q = 0.873$ Å^{-1}. The in-plane branches rigorously have either shear horizontal or longitudinal acoustic polarization along this high-symmetry axis. Furthermore, the two branches have equal frequencies at the Γ and K points, so that only one entry is needed for each approximation. Also listed are the mean-square amplitudes of vibration, in Å^2, evaluated by the QHT and SCP approximations. The ISCP entries for frequencies and the SCP entries for mean-square vibration amplitudes are thought to be the ''best estimates'' of those quantities.

T (K)		0	25	50	80
z	QHT	3.341	3.346	3.357	3.374
	SCP	3.344	3.351	3.366	3.385
$\omega_{0\parallel}$	QHT	1.28	1.28	1.27	1.25
	QHPT	1.27	1.25	1.20	1.13
	SCP	1.25	1.23	1.20	1.16
	ISCP	1.24	1.22	1.18	1.11
$\omega_{0\perp}$	QHT	3.60	3.56	3.48	3.33
	QHPT	3.60	3.55	3.44	3.43
	SCP	3.68	3.63	3.58	3.52
	ISCP	3.61	3.54	3.40	3.38
$\Delta\omega_\parallel$	QHT	0.39	0.39	0.40	0.40
	ISCP	0.47	0.59	0.58	0.71
$(\delta z)^2$	QHT	0.0043	0.0063	0.0114	0.0191
	SCP	0.0043	0.0064	0.0114	0.0181
$(\delta r_\parallel)^2$	QHT	0.022	0.061	0.120	0.194
	SCP	0.0202	0.0511	0.0880	0.1275

changes in the overlayer height cause changes in $\omega_{0\perp}$ and in the zone-center gap $\omega_{0\parallel}$ of the commensurate layer. Thus the finite-temperature forms of the QHPT and SCP approximations are required. The height z_{QHT} that minimizes the quasiharmonic free energy is used as the reference point in the QHPT calculation at the given temperature; it is very close to the height calculated in the SCP approximation, as shown in Table I.

The perturbation theory for the Xe/Pt(111) case is more complex than that for a 3D solid. When thermal expansion of the overlayer height is included, the expansion relative to the harmonic Hamiltonian includes first-order as well as third- and fourth-order terms in the displacement. The second-order perturbation correction ω_2 to the frequency includes the first-derivative terms. The consistency of the procedure is tested by calculating the perturbation shift δz in the average height from z_{QHPT} using linear and cubic terms. The contributions are nearly offsetting, and most of the remainder comes from a cubic anharmonic mixing of z and lateral motions that was not included in the calculation of the thermal expansion. Even so, there are no energy-conserving three-phonon processes to give a lifetime (broadening) of the in-plane modes. While one might extend the treatment of the quartic (four-phonon) process to second order in perturbation theory, a more promising route is to use molecular dynamics simulations to estimate the further processes.
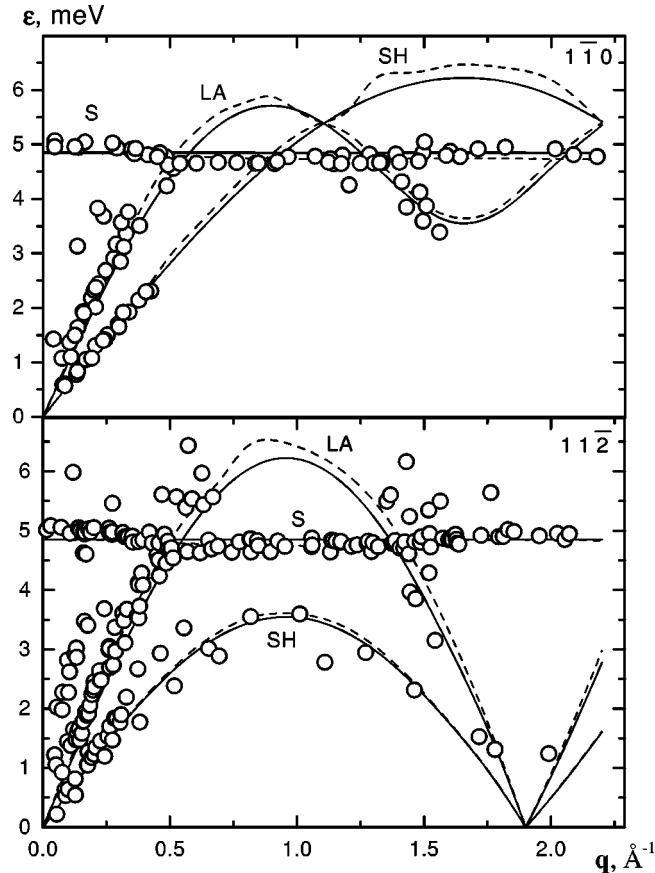
FIG. 1. Dispersion relations for the phonons of a monolayer solid of Ar/Pt(111) along the $[11\bar{2}]$ (ΓM) and $[1\bar{1}0]$ (ΓK) azimuths. The data, Ref. 8, are for a triangular lattice with $L = 3.79$ Å at 23 K. The calculated curves are the results of harmonic lattice dynamics (QHT—solid lines) and of quasiharmonic perturbation theory (QHPT—dashed lines) at 23 K for an interaction model consisting of the HFD-B2 pair potential augmented by the McLachlan substrate-mediated dispersion energy. The three branches are labeled by their polarizations: LA for longitudinal acoustic, SH for shear horizontal, and S for the vibration perpendicular to the monolayer plane.

The temperature-dependent SCP theory is reviewed in Ref. 1. The SCP frequencies are the solution to a variational harmonic approximation of the Helmholtz free energy in which the force constants are correlated Gaussian averages of the terms used in the QHT approximation.[16] The self-consistent determination of the vibrations has a more significant influence on the in-plane motions than on the z motions, as shown by the comparison in Table I of mean-square vibrations calculated in the SCP and QHT approximations.

III. INCOMMENSURATE MONOLAYER SOLID: Ar/Pt(111)

The QHT and QHPT results for the Ar/Pt(111) phonon dispersion curve at 23 K and $L = 3.79$ Å are compared to the results[8] of inelastic HAS experiments in Fig. 1. The previous identification of the experimental phonon branches with the shear horizontal (SH) and longitudinal acoustic (LA) monolayer modes was made on the basis of comparing to the results of the harmonic (QHT) approximation, and that iden-

tification is maintained when the anharmonic corrections are included. The slight irregularity in the QHPT results for the LA branch near 1 Å^{-1} along the $[11\bar{2}]$ azimuth arises from the second-order cubic anharmonic terms and might well be reduced in a self-consistent calculation.

A detailed comparison of the approximations for several wave vectors is presented in Ref. 16. At 0 K, the increment $\omega(\text{SCP}) - \omega(\text{QHT})$ agrees with the $\omega_1(4)$ term in the QHPT frequency to within 3% for both the SH and LA branches at all the wave vectors tested. Hence, the QHPT approximation is used for the comparisons to the experimental data in Fig. 1. The contributions of $\omega_1(4)$ and $\omega_2(3)$ significantly offset each other over most of the wave number range. The net effect in the SH branch, apparently the better-determined case of the Ar/Pt(111) dispersion curves, is smaller than present uncertainties of 0.2–0.3 meV in the experimental data. The corresponding terms for the 3D solid of Ar are significant in tests of interaction models because of the greater accuracy, better than 0.05 meV, in the inelastic neutron scattering measurements of the dispersion relations.[22]

The calculations presented in Fig. 1 include the McLachlan adsorption-induced dispersion energy. However, the frequency shifts for Ar/Pt(111) from the McLachlan term are less than 0.25 meV in the LA branch and less than 0.2 meV in the SH branch. Thus, comparisons to the data do not give strong evidence for the presence of this term.

The QHPT linewidths (lifetimes) follow an anticipated pattern. The SH frequency of QHT is a concave function of the wave number and hence the SH branch is intrinsically stable. Its linewidth arises from scattering by thermally excited phonons rather than from processes involving spontaneous and stimulated emission of phonons. At 23 K the largest width (HWHM) in the first Brillouin zone is 0.22 meV at $Q = 0.4$ Å^{-1} along the Γ–K azimuth, but for most of the Q range from Γ to K and to M, the width is small, $\Delta(\text{HWHM})/\omega(\text{SH}) < 0.05$. For the LA branch, spontaneous three-phonon decay processes are possible and except for wave vectors close to the Γ point, the dominant processes involve spontaneous and stimulated modes of decay rather than the scattering from thermally excited phonons. At 23 K the half-widths are mostly in the range $\Delta(\text{HWHM})/\omega(\text{LA}) \approx 0.05$–0.1.

IV. Xe/Pt(111)

In earlier work,[7] the harmonic lattice approximation to the phonon dispersion relations of the $\sqrt{3}R30°$ Xe/Pt(111) lattice was evaluated. The force constants of the Xe-Pt interaction were evaluated at the zero-temperature overlayer distance $z_0(\text{QHT})$. Surprisingly, the SH and LA branches are nearly degenerate in the QHT approximation for both the Γ–M and Γ–K azimuths of the xenon Brillouin zone. The frequency differences for given wave vectors are at the level of 0.1 meV and are smaller than the present resolution in the atomic scattering experiments. To fit the HAS data better, it was suggested to adjust the Barker-Rettner potential surface by lowering $\omega_{0\perp}$ from 3.6 meV to 3.4 meV and increasing $\omega_{0\parallel}$ from 1.3 meV to 1.6–1.7 meV.

The present work shows that there are rather large anharmonic shifts in the phonon frequencies. At 80 K, the anharmonic shifts lead to differences between the SH and LA

ε, meV
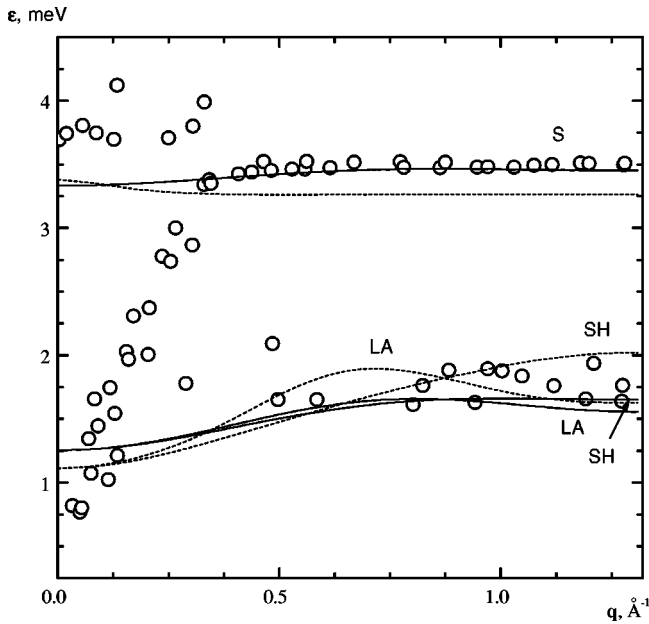
FIG. 2. Dispersion relations for the phonons of the commensurate $\sqrt{3}R30°$ Xe/Pt(111) lattice along the Γ–K–M azimuth. The data, Ref. 7, are for a triangular lattice with $L = 4.80$ Å at 80 K. The calculated curves are the results of harmonic lattice dynamics (QHT—solid lines) and the self-consistent-phonon approximation with cubic anharmonic corrections (ISCP—dashed lines). The interaction model consists of Xe-Xe interactions formed from the HFD-B2 potential with the McLachlan correction and the Barker-Rettner Xe-Pt potential energy surface. The curves at about 3.5 meV denote the S branch. At 1 to 2 meV, the curves are labeled by their polarizations, SH and LA. The steeply rising line of data points for Q in the range 0.1 to 0.3 Å^{-1} is the platinum Rayleigh mode.

frequencies of order 0.5 meV for wave vectors near the boundary of the first Brillouin zone; thus there are observable differences at the current level of experimental resolution. The anharmonic frequency corrections at 80 K are so large that calculation to an accuracy of better than 0.1 meV is still not assured. However, because the Brillouin-zone-center gap is large, $\omega_{0\parallel} > 1$ meV, there are no energy-conserving three-phonon decay processes for modes with polarization vectors in the plane of the monolayer, and hence they do not contribute to the phonon lifetime.

A. Commensurate Xe/Pt(111)

Results of the QHT and ISCP approximations to the SH and LA branches of the phonon dispersion relation are shown in Fig. 2 for $T = 80$ K. The Barker-Rettner Xe-Pt potential energy surface is used and the McLachlan term is included in the construction of the force constant matrix, although it is not a large contribution. The entries in Table I are less than complete characterizations of the dispersion relations but span the temperature range from 0 K to 80 K and demonstrate that the anharmonic effects increase so rapidly at temperatures above 50 K that the QHT results miss important features of the spectra at 80 K.

The overall trend shown in Fig. 2 is that the anharmonic terms increase the magnitude of the dispersion between the SH and LA branches near the Brillouin-zone boundary. Most

of the HAS data are at $Q > 0.5$ Å^{-1}. Even though the present calculations have reduced $\omega_{0\parallel}$, the increases near the zone boundary have the effect that the agreement with the experimental data remains satisfactory. There is no evident need for the *ad hoc* increase of $\omega_{0\parallel}$ made in Ref. 7 to improve the fit to the data. The comparison of the ISCP results to the experimental data in Fig. 2 suggests that both the LA and SH branches were detected in the HAS experiment,[7] as occurred also in a later experiment[8] on incommensurate monolayers.

The results in Table I from the four approximations (QHT, QHPT, SCP, and ISCP) can be used to recover the ω_1 and ω_2 in Eqs. (1.1) and (1.2). As expected, the size of these terms increases rapidly with increasing temperature and there is substantial cancellation between them. The zone-center gap $\omega_{0\parallel}$ decreases with increasing temperature, both because of the increase of z and because of the increasing anharmonicity. The effects of the anharmonicity are most pronounced in the frequency dispersion, which depends on the relative motion of atoms. Comparison of the mean-square in-plane displacements $(\delta r_\parallel)^2$ calculated with the QHT and SCP approximations suggests, as found by the more detailed comparisons, that $\omega_1(4)$ is an overestimate of the leading anharmonic shift. As the best estimate for the calculated dispersion curve to compare with the experimental data, we use the ISCP approximation, even though the cubic anharmonic term ω_2 is not determined self-consistently.

The zone-center gap for in-plane motions of the commensurate lattice decreases with increasing temperature, Table I. At 100 K, very close to the melting temperature of the solid, it is still larger than 1.1 meV; thus there is probably no ''floating solid'' at the commensurate lattice constant 4.80 Å with free translations of the center of mass along the substrate plane.

The values of $\omega_\perp$ at 80 K run 0.1–0.2 meV below those of the QHT theory, so that the reduction in the Xe-Pt force constant resulting from thermal expansion in z accounts for most of the reduction of $\omega_{0\perp}$ to 3.4 meV that was suggested[7] to better fit the 80-K data.

B. The S mode of incommensurate Xe/Pt(111)

The calculated values of the S-mode frequency $\omega_\perp$ highlight a remarkable feature of the experimental data that has not been emphasized in previous work. The frequency $\omega_\perp$ of incommensurate Xe/Pt(111) ($L \simeq 4.33$ Å) is reported to be[20] in the range 3.70–3.35 meV (using data at the Γ and K points) at 25 K and to be[8] about 3.4 meV at 50 K. Further, both in the commensurate $\sqrt{3}R30°$ Xe/Pt(111) lattice[7] and in a dilute 2D gas[8] of Xe on Pt(111) at 105 K the values are $\omega_\perp \simeq 3.5$ meV. However, the average adatom environments for the 2D gas and the incommensurate layer are generally considered to be quite different from the adsorption at an atop site for the commensurate lattice. At 80 K, the value of $\omega_{0\perp}$ calculated[16] for the laterally averaged Xe/Pt(111) potential is 2.20 meV, 1.2 meV smaller than the value for the commensurate Xe lattice. Thus the measured frequencies, for what are believed to be quite different circumstances, are much more similar than simple model calculations would indicate. A reduction in $\omega_\perp$, driven by a change in the overlayer height, of a few tenths of an meV (a few kelvins) is

anticipated for a temperature increase from 50 K to 100 K. This shift is close to present limits on experimental resolution.

There is another process that should lead to differences between $\omega_\perp$ of the commensurate solid and the 2D gas. In both cases the adsorbate mode is embedded in a continuum of substrate modes, so there may be hybridization with the substrate modes and shifting and damping of the adsorbate resonance. Data for the incommensurate solid have been discussed as an example of this process.[20] The corresponding theory[23] for the 2D gas treats the lifetime but not the frequency shift of the mode.

If the formulation of the hybridization theory of Ref. 24 is used for the monolayer solid, the shift $\delta\omega_\perp$ varies by about 0.33 meV across the Brillouin zone, while the dispersion from the adatom-adatom interactions is about 0.1 meV. The frequency shift for the single isolated adatom is ill-defined in the elastic substrate theory of Ref. 23. If the wave number at the 2D substrate surface Brillouin zone is taken as a cutoff in the theory, the shift from the unperturbed frequency is -0.4 meV.

These estimated shifts are all near the current level of experimental resolution for measuring $\omega_\perp$. However, the difference from the frequency calculated for the lateral average of the holding potential is so large that the conclusion appears to be that the experimental data for $\omega_\perp$ show that most of the xenon is at atop sites. This is a very different picture than the floating solid picture used to model the incommensurate solid and the low-density gas nearly free of lateral forces used to model the quasielastic helium atom scattering[21] of the 2D gas at 105 K.

V. CONCLUDING REMARKS

The agreement between the various approximations for the lattice dynamics of the Ar/Pt(111) monolayer leads to the conclusion that one can reliably evaluate the dispersion curve to a precision of 0.1 meV. In spite of the light mass, the net effect of the anharmonic terms is rather small, although they lead to lifetimes (linewidths) that may be resolved in future experiments.

On the other hand, the dilated lattice of the $\sqrt{3}R30°$ Xe/Pt(111) monolayer has rather small force constants for relative displacements of the adatoms and large anharmonic effects at 80 K, the temperature of recent measurements.[7] The anharmonic terms increase the frequency of the SH mode over most of the Brillouin-zone, generally by 10% to 20%. The percentage increases are much larger for the LA mode and raise the prospect that the perturbation theory is inadequate for an accurate calculation of the frequency. It appears that there is a difference of order 0.5 meV between the SH and LA branches near the Brillouin zone boundary. Comparing to the data suggests that both branches were detected in the experiment.

In a previous analysis of the HAS data for commensurate xenon,[7] it was suggested that the value of $\omega_{0\perp}$ be reduced from the 3.60 meV of the Barker-Rettner model (0 K) to 3.40 meV to better fit the data. As discussed in Sec. IV A, there are temperature-dependent anharmonic frequency decreases of order 0.2 meV caused by thermal expansion and it is no longer evident that the adjustment is necessary. If $\omega_\perp$ in the

incommensurate layer were determined by a lateral average of the Xe-Pt potential, there would be much larger frequency differences between the commensurate and incommensurate solid, but the measured values of $\omega_\perp$ are actually quite similar. The similarity is not understood at present.

Our calculation gives further evidence that the Barker-Rettner model is the best available potential surface for Xe/Pt(111), but, besides the question just discussed of the similarity of $\omega_\perp$ in different surface phases, there are two unresolved challenges to it arising from the fact that it is a quite corrugated surface. First, the corrugation is large enough that the nature of the ground-state structure of monolayer xenon in this potential is not evident. Our exploratory calculations indicate that the structure of lowest energy is a strongly modulated incommensurate solid. Second, a quasielastic scattering experiment[21] to measure in-plane mobility of dilute gaseous xenon found no detectable effect of the corrugation, although a simulation indicated there should have been one for motion on this surface.

Both the reliable calculation of frequencies in the xenon solid at 80 K and near its melting temperature and the phonon lifetime are questions that might be addressed with a molecular dynamics evaluation of the spectrum of lattice vibrations. Two features enhance the prospects for such an application: Temperatures of 70 to 100 K are high enough that the classical mechanics approximation should be accurate and the Xe-Pt potential energy surface of Barker and Rettner has had enough successful tests to warrant the investment of effort that would be required.

ACKNOWLEDGMENT

APPENDIX: DYNAMICS OF A LATTICE OF POLARIZABLE DIPOLES

The commensurate Xe/Pt(111) lattice is so dilated relative to the spacings in 3D solid xenon that one must reconsider contributions to the adatom-adatom forces that are usually thought to be negligibly small. One such process is the repulsive interactions between the adsorption-induced xenon electrostatic dipole moments. The presence of the moments is shown by changes in the work function of the metal. However, the interpretation of the work-function changes is complex because there are large depolarizing fields on an adatom from the moments on the other adatoms and the screening charges of the metal also make large contributions to the effective interactions of the adatom dipoles.[25] For Xe/Pt(111), the available information consists of the reported 0.65-eV change in the work function by the monolayer[26] and the 3.4-Å distance of Xe to the nearest surface Pt atom.[27] While the calculation of the depolarizing and screening fields is straightforward for a uniform adatom lattice, experiments do not give very strong support to the modeling.[28] Nonetheless, in this Appendix we estimate the contribution of the adsorption dipoles to the dispersion curves by evaluating the contributions to the monolayer elastic constants with such a model. The result is that the terms contribute approximately 0.1 meV to the frequencies near the Brillouin-zone boundary

and are much smaller through most of the Brillouin zone. Thus they are on the order of, or less than, the present experimental accuracy and do not affect the conclusions reached in the text. This analysis has a basic significance because the depolarizing fields amount to many-body forces and the elastic constant contributions do not follow the Cauchy conditions for a triangular lattice.

The electric field at site i from a dipole $\vec{p}_j$ at site j is

$$\vec{E}_i(j) = -\frac{I - 3\hat{R}_{ij}\hat{R}_{ij}}{R_{ij}^3} \cdot \vec{p}_j. \qquad (A1)$$

The self-consistency equation determining the dipole moment at site i is

$$\vec{p}_i = \vec{p}_0' + \alpha \vec{E}_i(i') + \alpha \sum_{j(\neq i)} [\vec{E}_i(j) + \vec{E}_i(j')], \qquad (A2)$$

where α is the polarizability of the adatom, the prime on the site index denotes the electrostatic image (equivalent to the substrate screening charges) of the dipole at that site, and $\vec{p}_0'$ is the dipole moment of an isolated adatom without the self-image contribution. That is, the dipole moment (perpendicular to the substrate) on the adatom at very low coverage is

$$p_0 = p_0'/[1 - (\alpha/4l^3)], \qquad (A3)$$

using the distance l from the adatom to the effective electrodynamic surface of the substrate. Solving the self-consistency equation and calculating the energy to assemble a monolayer lattice of dipoles leads to the Topping formula.[25] Here the substrate screening charges increase both the interaction energy and the effective polarizability of the adatom.

For a monolayer configuration with a general set of in-plane displacements from the triangular lattice, the self-consistency equation Eq. (A2) leads to components of dipole moment parallel as well as perpendicular to the surface. However, in the approximation that the lateral distances to the dipole moments are large compared to the perpendicular distance $2l$ to the plane of the image dipoles, the parallel component is zero. We assume this to be valid for the Xe/Pt(111) monolayer and then find that the self-consistency equation is a scalar equation for the z component of the dipoles:

$$[1 - (\alpha/4l^3)]p_i = p_0' - 2\alpha \sum_{j(\neq i)} p_j/R_{ij}^3. \qquad (A4)$$

The elastic constants are determined as the coefficients of second-order terms in the expansion of the assembly energy in powers of the Lagrangian strain tensor.[29] Define the dipole moment at monolayer coverage to be p_f, the area per ada-

tom in the triangular lattice to be $a_c = L^2\sqrt{3}/2$, with L the nearest-neighbor spacing, and a lattice sum $A_3 \approx 11.03 \ldots$. The relation to the ''bare'' moment is $p_f = p_0'/f$ with

$$f = [1 - (\alpha/4l^3)] + (2\alpha A_3/L^3). \qquad (A5)$$

The contributions to the 2D pressure $\delta\phi$ and bulk modulus δB are

$$a_c \delta\phi = \frac{3A_3 p_f^2}{L^3}; \qquad (A6)$$

$$a_c \delta B = \frac{A_3 p_f^2}{L^3}\left[\frac{15}{4} - \frac{9\alpha A_3}{fL^3}\right]. \qquad (A7)$$

The elastic constants C_{11}, C_{12}, C_{33}, in Voigt notation, are related by

$$C_{11} = C_{12} + 2C_{33}; \qquad (A8)$$

$$B = C_{12} + C_{33}. \qquad (A9)$$

For pair potentials, the elastic constants follow the relation for a Cauchy solid, $C_{12} = C_{33}$, and determining the bulk modulus is sufficient to construct the speeds of the elastic waves. However, the depolarizing fields break the Cauchy relation and the contributions from the dipoles are

$$a_c \delta C_{12} = \frac{A_3 p_f^2}{L^3}\left[\frac{15}{8} - \frac{9\alpha A_3}{fL^3}\right]; \qquad (A10)$$

$$a_c \delta C_{33} = \frac{A_3 p_f^2}{L^3}\left[\frac{15}{8}\right]. \qquad (A11)$$

The contributions in the squared speeds of longitudinal and transverse sound for the triangular lattice of atoms of mass m are

$$m\delta c_l^2 = a_c[\delta C_{11} - \delta\phi]; \qquad (A12)$$

$$m\delta c_t^2 = a_c[\delta C_{33} - \delta\phi]. \qquad (A13)$$

The work-function change[26] of 0.65 eV corresponds to a dipole moment $p_f = 0.32$ D in the lattice with $L = 4.8$ Å. The xenon polarizability is $\alpha = 4.0$ Å^3 and the distance $l = 2.0$ Å. Then $f = 1.50$ and at $q = 1.0$ Å^{-1}, the added piece in the squared frequency is 0.26 meV^2 for the LA branch, or an increase of less than 0.1 meV in ω (LA) at $q = 1.0$ Å^{-1}. In the SH branch the effect is about 3 times smaller. With these parameters the dipole contribution to C_{12} is negative, an unusual circumstance but one that does not appear to violate any general requirements on the elastic constants of a triangular lattice.

[1] A. D. Novaco, Phys. Rev. B **19**, 6493 (1979); **46**, 8178 (1992).

[2] T. M. Hakim, H. R. Glyde, and S. T. Chui, Phys. Rev. B **37**, 974 (1988).

[3] A. P. Graham, M. F. Bertino, F. Hofmann, J. P. Toennies, and Ch. Wöll, J. Chem. Phys. **106**, 6194 (1997); **107**, 4445 (1997).

[4] J. Braun, D. Fuhrmann, A. Šiber, B. Gumhalter, and Ch. Wöll, Phys. Rev. Lett. **80**, 125 (1998).

[5] R. Gerlach, A. P. Graham, J. P. Toennies, and H. Weiss, J. Chem. Phys. **109**, 5319 (1998); Rolf Gerlach, Diplom thesis, University of Göttingen (1994).

[6] A. Šiber, B. Gumhalter, J. Braun, A. P. Graham, M. Bertino, J. P. Toennies, D. Fuhrmann, and Ch. Wöll, Phys. Rev. B **59**, 5898 (1999).

[7] L. W. Bruch, A. P. Graham, and J. P. Toennies, Mol. Phys. **95**, 579 (1998).

[8] L. W. Bruch, A. P Graham, and J. P. Toennies, J. Chem. Phys. (to be published).

[9] L. W. Bruch, J. Chem. Phys. **107**, 4443 (1997).

[10] A. A. Maradudin, E. W. Montroll, G. H. Weiss, and I. P. Ipatova, *Theory of Lattice Dynamics in the Harmonic Approximation* (Academic, New York, 1971).

[11] H. R. Glyde and M. G. Smoes, Phys. Rev. B **22**, 6391 (1980), and references contained therein.

[12] The examples are triangular lattices with nearest neighbor spacing denoted L.

[13] *Rare Gas Solids*, edited by M. L. Klein and J. A. Venables (Academic, New York, 1976), Vol. I; (Academic, New York, 1977), Vol. II.

[14] L. W. Bruch, M. W. Cole, and E. Zaremba, *Physical Adsorption: Forces and Phenomena* (Oxford University Press, New York, 1997).

[15] M. L. Klein and T. R. Koehler, in *Rare Gas Solids*, edited by M. L. Klein and J. A. Venables (Academic, New York, 1976), Vol. I, p. 316. Our implementation of the ISCP differs from the standard form by not having Gaussian averages of the derivatives of the potential in the cubic term.

[16] See EPAPS Document No. E-PRBMDO-61-017008 for more details of the calculations and tables showing detailed comparisons of the successive stages of approximation. This document may be retrieved via the EPAPS homepage (http://www.aip.org/pubservs/epaps.html) or from ftp.aip.org in the directory /epaps/. See the EPAPS homepage for more information.

[17] R. A. Aziz and M. J. Slaman, Mol. Phys. **58**, 679 (1986); A. K. Dham, W. J. Meath, A. R. Allnatt, R. A. Aziz, and M. J. Slaman, Chem. Phys. **142**, 173 (1990).

[18] J. A. Barker and C. T. Rettner, J. Chem. Phys. **97**, 5844 (1992); **101**, 9202(E) (1994).

[19] V. N. Kashcheev and M. A. Krivoglaz, Fiz. Tverd. Tela (Leningrad) **3**, 1528 (1961) [Sov. Phys. Solid State **3**, 1107 (1961)]; A. A. Maradudin and A. E. Fein, Phys. Rev. **128**, 2589 (1962). The one-phonon response function is evaluated using the retarded Green's function $\langle\langle a_k; a_k^{\dagger}\rangle\rangle$, where a_k and $a_k^{\dagger}$ are annihilation and creation operators for the oscillator mode k. The Green's-function hierarchy is decoupled and the frequency shift and linewidth are derived from the resulting Lorentzian line shape.

[20] B. Hall, D. L. Mills, P. Zeppenfeld, K. Kern, U. Becher, and G. Comsa, Phys. Rev. B **40**, 6326 (1989).

[21] J. Ellis, A. P. Graham, and J. P. Toennies, Phys. Rev. Lett. **82**, 5072 (1999).

[22] Y. Fujii, N. A. Lurie, R. Pynn, and G. Shirane, Phys. Rev. B **10**, 3647 (1974).

[23] B. N. J. Persson, E. Tosatti, D. Fuhrmann, G. Witte, and Ch. Wöll, Phys. Rev. B **59**, 11 777 (1999).

[24] L. W. Bruch and F. Y. Hansen, Phys. Rev. B **55**, 1782 (1997).

[25] B. L. Maschhoff and J. P. Cowin, J. Chem. Phys. **101**, 8138 (1994), and references contained therein.

[26] G. Schönhense, Appl. Phys. A: Solids Surf. **41**, 39 (1986).

[27] Th. Seyller, M. Caragiu, R. D. Diehl, P. Kaukasoina, and M. Lindroos, Phys. Rev. B **60**, 11 084 (1999).

[28] See, for instance, the variation of the work function with coverage reported for Xe/Pd(100) by E. R. Moog and M. B. Webb, Surf. Sci. **148**, 338 (1983).

[29] See the formulation in L. W. Bruch and J. M. Gottlieb, Phys. Rev. B **37**, 4920 (1988).